Astron. Astrophys. 338, 599–611 (1998)

ASTRONOMY
AND
ASTROPHYSICS

On the nature of apparent changes of the orbital period in symbiotic binaries

A. Skopal[1,2]

[1] Astronomisches Institut der Universität Erlangen-Nürnberg, Sternwartstr. 7, D-96049 Bamberg, Germany
[2] Astronomickýústav, Slovenská akadémia vied, 059 60 Tatranská Lomnica, Slovakia (astrskop@auriga.ta3.sk)

Received 29 April 1998 / Accepted 27 July 1998

Abstract. We present long-term photometric observations of a group of classical symbiotic stars: BF Cyg, CI Cyg, V1329 Cyg, AG Peg, Z And, AG Dra and YY Her. Analysis of the minima positions in the historical light curves revealed a systematic variation in the $O-C$ residuals which indicates apparent changes of the orbital period in these systems. It was found that (i) this variation is connected with changes in the energy distribution of the hot star spectrum, and (ii) the phase shift in the period correlates with the change in the star's brightness. The effects are best demonstrated by the eclipsing systems of BF Cyg and CI Cyg. During quiescent phases, when the nebular radiation dominates the optical spectrum, the minima occur prior to the time of the inferior conjunction of the giant star. However, during active phases, when the component of recombination radiation decreases considerably and a cool shell around the hot star developes, the minima – eclipses – coincide with spectroscopic conjunction of the stars.

The observed variation is interpreted as a result of systematic changes in both geometry and location of the main source of the optical continuum caused by a variation in the luminosity of photons capable of ionizing hydrogen during transition periods between different levels of activity of symbiotic binary.

Key words: stars: binaries: symbiotics – circumstellar matter – stars: fundamental parameters

1. Introduction

Symbiotic stars represent a group of objects characterized by the simultaneous presence of two extremely different temperature regimes. The cooler is that of an M-giant spectral type, and the hotter is expressed by a hot star continuum ($T_\star \approx 10^5$ K) and emission lines of high excitation, such as HI, HeII, [FeVII], [OIII], [NeIII], etc. At present, they are commonly accepted as long-period interacting binary systems ($P_{\rm orb} \approx 1-3$ years) consisting of a red giant and a hot compact component, embedded in a gaseous nebula. Many systems show phases of intense activity alternating with extended quiescent periods.

During *quiescent phases*, the hot star radiation ionizes a portion of the neutral circumbinary material giving rise to the hydrogen recombination continuum which often dominates the near-UV and the optical spectrum (e.g. Nussbaumer & Vogel 1989; Fernandez-Castro et al. 1990). The geometry of the optically thick part of the HII region determines the observed shape of the light curve (LC). Generally, we observe a periodic wave-like variation as a function of the orbital phase. A simple quantitative model of the structure of the ionized hydrogen in symbiotic systems for a steady state situation was first introduced by Seaquist, Taylor & Button (1984). Their model has been very successful in explaining the radio properties of symbiotic stars. However, recent hydrodynamical calculations of the interaction of the stellar winds including effects of the orbital motion (e.g. Walder 1995) suggest a rather complex asymmetrical structure of the HII region in symbiotic stars.

During *active phases* the hot component expands in radius and becomes significantly cooler. A mass-outflow from the active star is indicated directly by a broadening of emission lines and/or by profiles of the P-Cygni type. This results in a suppression of the HII zone. The source of the optical light is restricted mostly to the hot component (pseudo)photosphere. The wave-like variation disappears, and in the case of a high inclination of the orbital plane, a deep narrow minimum in the LC, caused by an eclipse of the hot component by its giant companion, is observed. In addition, an increase in the star's brightness, typically by 2-3 mag, on the time-scale of weeks, followed by a gradual decrease into quiescence within a few years, represents the most impressive face of active stages.

The very different geometry of the source of the optical light during different levels of activity can be seen well in the profiles of LCs (e.g. Skopal 1995, 1996, 1998). Also variation in the minima positions has been reported for different objects by many authors (see below Sect. 3.1). However, all authors assumed that measurement errors are the only source of variability in the data. The main aim of this contribution is to demonstrate these changes and to suggest their possible nature. In Sect. 3, we show that a transition between different levels of activity produces a systematic variation in the $O-C$ residuals and thus an apparent change in the orbital period. In Sect. 4, we suggest a descriptive model explaining the nature of these observations.

2. Method of treatment

To explore variation in LCs of symbiotic binaries caused by a transition from an active to a quiescent phase, or vice versa, we do need long-term photometric observations containing, at least, one active phase with a good coverage by the data. However, there are only few systems of which LCs fulfil this strong condition: BF Cyg, CI Cyg, V1329 Cyg, AG Peg, Z And, AG Dra and YY Her. To construct the LCs we used the data from the literature and also the visual magnitude estimates made by Association Francaise des Observateurs d'Etoiles Variables (AFOEV) which are available on CDS. There are two main reasons for using the visual data: (i) A continuous coverage of LCs, mainly during the recent observational seasons which are very poorly, if at all, covered by other data, and (ii) a good determination of a sudden change in the star's brightness. The merit of the visual observations is described in Skopal (1995).

We were searching for accurate positions of the observed minima to determine the location of the main emission source in the binary. We employed several methods with respect to the shape and the coverage of minima. Particularly, we used the methods of parabola fit, Kwee and Van Woerden method, sliding integration method, trace paper and "center of mass" methods, which are described in detail by Ghedini (1982). For the data published only in graphical form we made an estimate by eye, and/or we used already published mid-points of the minima. In most cases, uncertainties in the position of the minima were less than 10 days (no mark in tables). Uncertainties between about 10 and 20 days are marked by ':', and poorly defined minima with an uncertain position, by '::'.

An independent prediction of a specific position of the binary components, for example the time of the inferior conjunction of the cool star, is also required. We use the elements of the spectroscopic orbit, if they are available, otherwise we consider an average ephemeris of the minima derived from historical records of observations. We discuss this point below for individual objects separately. The uncertainties in periods resulting from timings of the minima were determined in a standard way (e.g. Batten 1973). Then we constructed the $O-C$ diagrams with respect to a 'firm' ephemeris. Results are summarized in Tables 1 to 7 and Figs. 1 to 11.

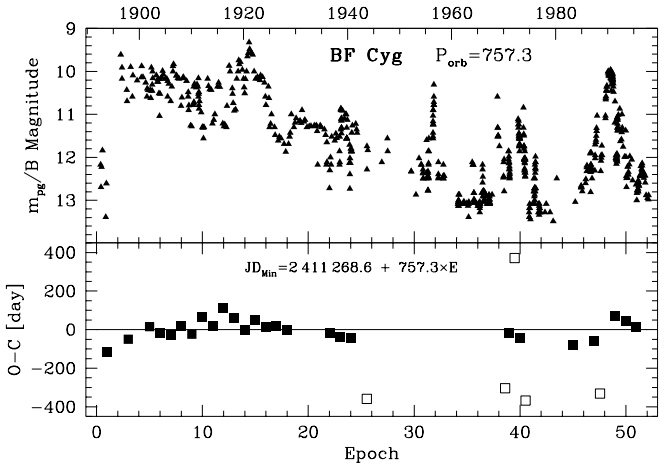

Fig. 1. Top: The historical LC of BF Cyg. Bottom: The $O-C$ diagram for the minima listed in Table 1. Full and open squares represent the primary and secondary minima, respectively

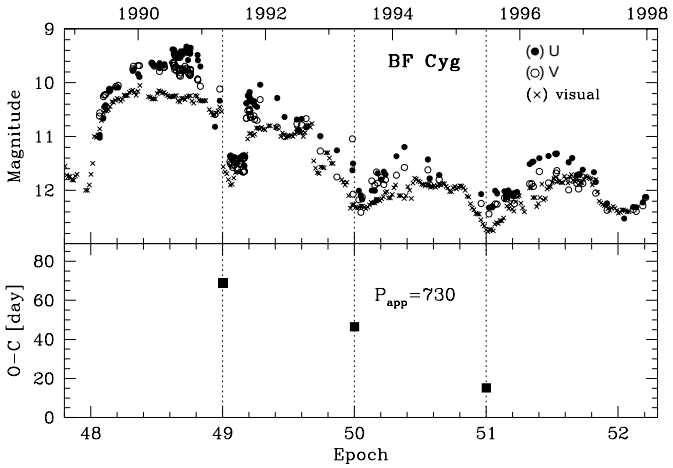

Fig. 2. Top: The U, V and visual (smoothed in 30-day bins) LCs of BF Cyg covering its recent active phase. The change in the shape and position of the minima during the $A \rightarrow Q$ transition is well illustrated. Bottom: Corresponding $O-C$ residuals indicate an apparent period of 730 days. The dotted vertical lines give the position of the calculated minimum.

3. Observational arguments

3.1. The objects

Here we summarize basic properties of the objects under consideration important for understanding the investigated variation in their LCs: (i) Fundamental parameters, (ii) main characteristics of the active and quiescent phases, (iii) the ephemeris for the orbital motion and, finally, we give (iv) a description of our observational results.

BF Cyg ($P_{\rm orb}$=757.3 days): Recent study suggested that the system consists of an M bright giant ($M_{\rm g} \sim 2\,{\rm M}_\odot$, $R_{\rm g} \sim 240-280\,{\rm R}_\odot$, $L_{\rm g} \sim 5\,000\,{\rm L}_\odot$) probably close to its Roche lobe, and a hot, compact object ($M_{\rm h} \sim 0.3-0.4\,{\rm M}_\odot$, $L_{\rm h} \sim 1.4\,L_{\rm g}$, $T_{\rm h}$(in quiescence)$\sim\ 8\times10^4$ K) with an orbital inclination $i \approx 70-90^\circ$ (Skopal et al. 1997).

During the 1989 active phase, an optically thick shell was ejected, the hot star temperature decreased to 18 000 – 12 000 K and the optical continuum was restricted to the hot star (pseudo) photosphere. We observed a deep minimum caused by an eclipse of the active component by its giant companion (cf. Skopal et al. 1997; Cassatella et al. 1992). On the other hand, during quiescent phase, the energy distribution in the spectrum shows a strong nebular component dominating the near-UV/optical and a hot stellar source in the far-UV region (e.g. Fernandez-Castro et al. 1990). A variable attenuation of the far-UV continuum due to Rayleigh scattering of the hot star light by the neutral hydrogen atoms of the cool giant wind was indicated by the IUE observations (Gonzalez-Riestra et al. 1990). During the

Table 1. Minima in the light curve of BF Cyg

JD_{Min} -2 400 000	Type	Ref	Phase*	E	O-C*
11910::	pg	1	0.847	1	-115.9
13490	pg	1	2.933	3	-50.5
15070	pg	1	5.020	5	14.9
15795	pg	1	5.977	6	-17.4
16540	pg	1	6.961	7	-29.7
17345	pg	1	8.024	8	18.0
18060	pg	1	8.968	9	-24.3
18910	pg	1	10.090	10	68.4
19620	pg	1	11.028	11	21.1
20470:	pg	1	12.150	12	113.8
21175	pg	1	13.081	13	61.5
21870	pg	1	13.999	14	-0.8
22680	pg	1	15.069	15	51.9
23400	pg	1	16.019	16	14.6
24160	pg	1	17.023	17	17.3
24900	pg	1	18.000	18	0.0
27910	pg	1	21.975	22	-19.2
28650	pg	1	22.952	23	-36.5
29400::	pg	1	23.942	24	-43.8
30600	pg	2	25.527	26	-358.4
40500	pg	2	38.599	39	-303.3
40785	pg,vis	2,3	38.976	39	-18.3
41175	vis	3	39.491	39	371.7
41520	pg	2	39.946	40	-40.6
41950	pg	2	40.514	41	-367.9
45268	vis	3	44.896	45	-79.1
46800:	UBV	2	46.919	47	-61.7
47288	vis	3	47.563	48	-331.0
48445.3	UBV,vis	2,3	49.091	49	68.7
49180:	V,vis	2,3	50.061	50	46.4
49906	UBV,vis	2,3	51.020	51	15.1

References: 1 - Jacchia (1941), 2 - from data referred in Skopal et al. (1997), 3 - from the AFOEV data on CDS
$\star$ JD_{Min} = 2 411 268.6 + 757.3×E

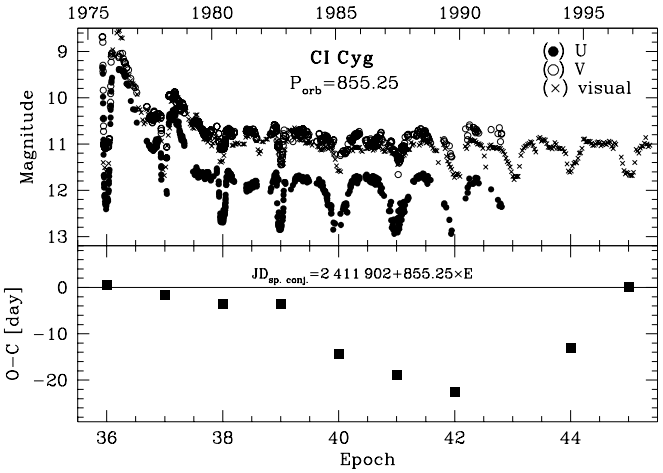

Fig. 3. The U, V and visual LCs of CI Cyg from its main outburst in 1975. Variation in the shape of the minima during the $A \rightarrow Q$ transition (top) is followed by a variation in their positions (bottom)

Table 2. Minima in the light curve of CI Cyg.

JD_{Min} -2 400 000	Type	Ref	Phase*	E	O-C*
42691.6	UBV	1	36.001	36	0.6
43544.7	UBV,vis	1,2	36.998	37	-1.6
44397.9	UBV,vis	1,2	37.996	38	-3.6
45253.1	UBV	1	38.996	39	-3.6
46097.6	UB	1	39.983	40	-14.4
46948.3	UBV	1	40.978	41	-18.9
47800.0:	U,vis	1,2	41.974	42	-22.5
48691.7:	vis	2	43.016	43	13.9
49520.0	vis	2	43.985	44	-13.0
50388.3	vis	2	45.000	45	0.1

References: 1 - Belyakina (1979, 1984, 1992), Hric et al. (1991, 1993), Skopal et al. (1992), 2 - from the AFOEV data on CDS
$\star$ JD_{Min} = 2 411 902 + 855.25×E

orbital cycle, 1986-89, the Rayleigh attenuation was seen from the orbital phase ∼0.9 to ∼1.6.

A very strong hot continuum masks absorption lines of the red giant in the optical and thus the orbital motions of the components are very poorly known (e.g. Mikolajewska et al. 1989). Therefore, for the purpose of this paper, we use the ephemeris derived from the primary minima (such that $|O-C| < 116$ days) in the historical LC (Table 1) as

$$JD_{\rm Min} = 2\,411\,268.6 + 757.3(\pm 0.6) \times E. \quad (1)$$

The period of 757.3 days is the same as that already derived by Pucinskas (1970) who supported this value also by periodic variations of other spectrophotometric parameters. We adopt this period as the orbital period of the binary motion.

Fig. 1 shows the historical LC with the $O-C$ diagram. Positions of the minima are given in Table 1. A systematic variation in the $O-C$ residuals is clearly seen. This behaviour was already noted by Jacchia (1941). An increase before the 1920 bright stage (E=1 to 11) corresponds to a period of 770 days, while the subsequent decrease (E=12 to 24) indicates a shorter period of 747.5 days. Skopal (1992) found that epochs of minima depend on the star's brightness, and generally ascribed this relation to an interaction of the circumstellar matter in the system. The same type of variability appeared again during the recent, 1989 active phase. Observed changes in both the position and the shape of the minima are illustrated in Fig. 2. During the transition *from the active phase to quiescence* (the $A \rightarrow Q$ transition), a systematic change in the minima positions at E=49 to 51 corresponds to a period of 730 days. During the transition *from the quiescent to the active phase* ($Q \rightarrow A$), a significant change in the $O-C$ values by jump of +130 days was observed. The minima at E=45 to E=49 indicate an apparent period of 794 days (Table 1, Fig. 2).

CI Cyg ($P_{\rm orb}$=855.25 days): The recent detailed study of CI Cyg made by Kenyon at al. (1991) suggests that this system contains an M5 II giant ($M_{\rm g} \sim 1.5\,{\rm M}_\odot$, $L_{\rm g} \sim 4\,500\,{\rm L}_\odot$) and a low mass main-sequence star ($M_{\rm h} \sim 0.5\,{\rm M}_\odot$, $L_{\rm h} \approx 1\,500\,{\rm L}_\odot$, $T_{\rm h} \sim 10^5$ K), with a high inclination of the orbit of $\sim 73°$.

Evolution of the LC from its major eruption in 1975 provides striking constraints on the structure and nature of the source of

the optical light. The narrow minima during the first four cycles from the maximum suggest the source of the optical continuum to be formed in a small volume (in the binary dimensions) centered on the hot star. Also the HeII and HI emissions were restricted to the region eclipsed by the giant (Kenyon et al. 1991). This implies that the nebular contribution was negligible at the maximum. Contrary to this behaviour, during subsequent cycles, the broad minima in both the continuum and the HI lines developed. The near-UV/optical spectrum was dominated by the nebular emission and the lines of highly ionized elements (Kenyon et al. 1991). Such evolution resembles that observed for BF Cyg, although it was slower and exhibited a much higher stage of excitation.

Whitney (see Aller 1954) derived the ephemeris for the times of minima as

$$JD_{\rm Min} = 2\,411\,902 + 855.25 \times E. \quad (2)$$

Belyakina (1979, 1984, 1992) confirmed this period with photoelectric photometry and clearly showed that CI Cyg is an eclipsing system. Positions of the deep eclipse at JD 2 442 692 and the last one, observed at JD 2 450 388, agree perfectly with their predictions by Eq. (2). Therefore we adopt the Whitney's ephemeris for the purpose of this paper, considering that this also represents timing of the inferior conjunction of the giant star in CI Cyg.

Fig. 3 shows the LC of CI Cyg in the U and V/visual bands covering the recent $A \rightarrow Q$ transition period. The $O-C$ residuals are listed in Table 2. Also here, more attempts to improve the photometric elements have been noted in the literature. Mikolajewska & Mikolajewski (1983) and Mikolajewska (1997) marginally modified Whitney's ephemeris, while Kenyon et al. (1991) suggested the orbital period to be 1-2 days shorter than 855.25 days, as the minima at E=37 to 39 (in our notation) occurred $\sim$5 days prior to the predictions of Whitney's ephemeris. Our results demonstrate qualitatively the same behaviour throughout the $A \rightarrow Q$ transition as in the case of BF Cyg. Minima observed during the nebular stage (from E=40 to 42) indicate a shorter period of 849 days. However, the last minimum (E=45) appeared to be more rectangular in shape and its position returned to that predicted by the ephemeris (2). Maybe CI Cyg is just preparing for a new activity.

V1329 Cyg ($P_{\rm orb}$=958 days): The fundamental parameters of this system are not well established at present. The binary consists of an M giant and a white dwarf ($L_{\rm h} \sim 950\,{\rm L}_\odot$, $T_{\rm h} \sim$145 000 K) with a high inclination of the orbit of $\sim 86 \pm 2^\circ$ (cf. Nussbaumer et al. 1986; Mürset et al. 1991; Schild & Schmid 1997).

The symbiotic phenomenon of V1329 Cyg developed in the 1964 outburst. The post-outburst LC shows large, $\sim$1.5 mag deep, periodic wave-like variations connected with the binary motion. The IUE observations revealed the presence of a strong nebulosity in the near-UV spectrum. It also varies along the orbit. Around the optical minima the UV continuum is flat and very faint, while at the maxima the near-UV fluxes are a factor of $\sim$5 stronger (cf. Fig. 2 and Table 4 of Nussbaumer & Vogel 1991).

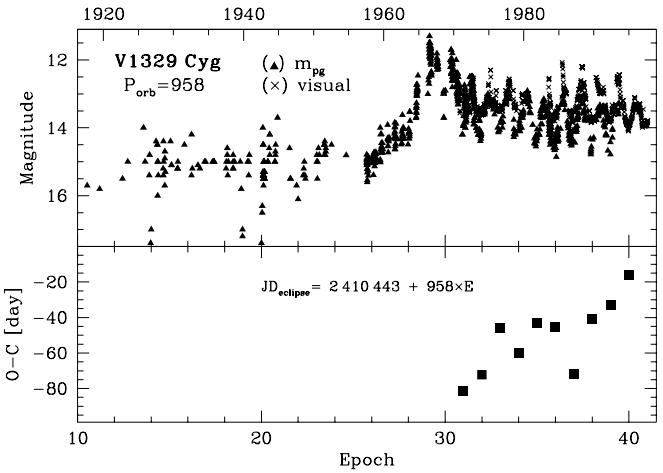

Fig. 4. The historical LC of V1329 Cyg with the $O-C$ diagram for the minima which developed during the symbiotic activity

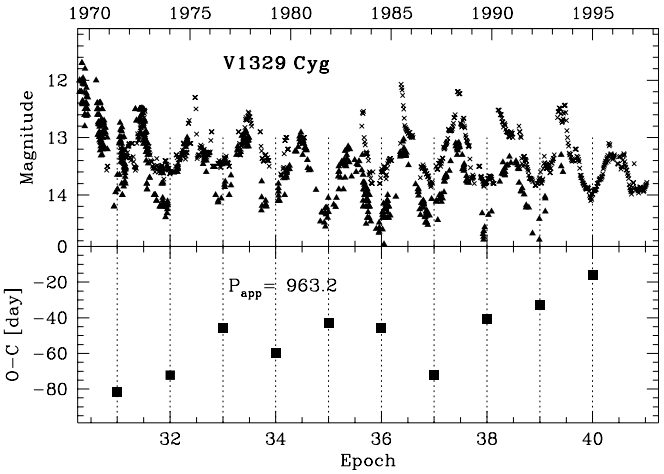

Fig. 5. Top: A part of the LC of V1329 Cyg covering its active phase. Bottom: A systematic increase in the $O-C$ values indicates an apparet period of 963.2 days

Before the 1964 outburst, V1329 Cyg was an inactive star of about 15th magnitude displaying $\sim$2 mag deep eclipses. Photometric variability from the pre-outburst period is well documented by Stienon et al. (1974), who suggested an orbital period of 959 days. Later re-analyses of Stienon's et al. (1974) data set argued for shorter periods between about 950 and 954 days (Grygar et al. 1979; Munari et al. 1988; Hric et al. 1993). The most recent careful re-analysis of the pre-outburst data made by Schild & Schmid (1997) revealed the ephemeris

$$JD_{\rm eclipse} = 2\,427\,687(\pm 20) + 958.0(\pm 1.8) \times E, \quad (3)$$

which we adopt for the purpose of this paper. In addition, as the data are not affected by any activity from that time, we also assume that this ephemeris is identical to that for the inferior conjunction of the giant star.

Fig. 4 shows the compiled photographic/visual LC from 1920. The times of minima are listed in Table 3. A sudden change in the star's brightness due to the eruption causes a sud-

Table 3. Minima in the light curve of V1329 Cyg.

JD_{Min} -2 400 000	Type	Ref	Phase*	E	O-C*
41017.4:	pg	1	31.915	31	-81.6
41984.7	pg,vis	1,3	32.925	32	-72.3
42969.2:	pg,vis	1,3	33.952	33	-45.8
43913.2	UBV,pg	2,1	34.938	34	-59.8
44887.8	UBV,pg	2,1	35.955	35	-43.2
45843.5	UBV,pg,vis	2,1,3	36.959	36	-45.5
46775.0	UB,pg	2,1	37.922	37	-72.0
47764.4	pg	1	38.958	38	-40.6
48730.0	pg,vis	1,3	39.966	39	-33.0
49705.0	vis	3	40.983	40	-16.0

References: 1 - Stienon et al. (1974), Arkhipova & Mandel (1973), Hric et al. (1993), 2 - Arkhipova (1977), Arkhipova & Ikonnikova (1989), 3 - from the AFOEV data on CDS

$\star$ $JD_{\rm eclipse}$ = 2 410 443 + 958.0×E

Table 4. Minima in the light curve of AG Peg

JD_{Min} -2 400 000	Type	Ref	Phase*	E	O-C*
28350	pg	1	0.844	1	-126.8
29060	pg	1	1.718	2	-229.4
29910	pg	1	2.764	3	-192.0
32550	pg	1	6.013	6	10.2
33200	pg	1	6.812	7	-152.4
34080	pg	1	7.895	8	-85.0
34880	pg	1	8.880	9	-97.6
35550	pg	1	9.704	10	-240.2
36630	pg	1	11.033	11	27.2
37380	pg	1	11.956	12	-35.4
38151.9	UBV	2	12.906	13	-76.1
38966.6	UBV,pg	2,1	13.909	14	-74.0
39812.5:	UBV	2	14.950	15	-40.7
40590::	pg	1	15.907	16	-75.8
41530:	pg	1	17.063	17	51.6
42276.1	UBV	2	17.982	18	-14.9
43101.6	UBV	2	18.998	19	-2.0
43875::	vis,pg	3,1	19.949	20	-41.2
44702.8	UBV	2	20.968	21	-26.0
45467.8	UBV	2	21.909	22	-73.6
47168.2	UBV	2	24.002	24	1.6
47968.5	UBV	2	24.987	25	-10.7
48851.6	vis	3	26.074	26	59.8
49690	vis	3	27.105	27	85.6
50459.3	vis	3	28.052	28	42.3

References: 1 - Meinunger (1983), 2 - determined from the published data (see text), 3 - from the AFOEV data on CDS

$\star$ $JD_{\rm sp.conj.}$ = 2 427 664.2 + 812.6×E

den change in the position of the subsequent minimum (E=31) by about -80 days. All minima occurred prior to the time of spectroscopic conjunction. The $O-C$ residuals systematically increase along the decrease of the star's brightness (see Figs. 4, 5), indicating a larger period than the orbital one. A linear regression of the minima in Table 3 yields their ephemeris as

$$JD_{\rm Min} = 2\,440\,061.6 + 963.2(\pm 0.9) \times E,$$

which, according to Eq. (3), sets the initial epoch of the post-outburst minima at the orbital phase ~ 0.92. Practically the same result, 963.3($\pm$0.7) days, was obtained by Hric et al. (1993), who applied a sine wave fit to the photographic data throughout 7 cycles. The two different periods in the pre- and post-outburst LCs, respectively, are also clearly identified by the Stellingwerf's (1978) method of phase minimization (cf. Hric et al. 1993). The shift between the position of the pre-outburst eclipses and the post-outburst minima is directly seen in Fig. 5.

AG Peg ($P_{\rm orb}$=812.6 days): This symbiotic star is composed of a normal M3 giant ($M_{\rm g} \sim 2.5\,{\rm M}_\odot$, $R_{\rm g} \sim 85\,{\rm R}_\odot$, $L_{\rm g} \sim 1\,150\,{\rm L}_\odot$) and a hot component ($M_{\rm h} \sim 0.6\,{\rm M}_\odot$, $L_{\rm h} \approx 5\,000 - 750\,{\rm L}_\odot$, $T_{\rm eff} \sim 10^5$ K) embedded in a dense ionized nebula (Kenyon et al. 1993). The star is classified as a symbiotic nova. In mid-1850's it rose in brightness from $\sim$9 to $\sim$6 mag and afterwards followed a gradual decline to the present brightness of $\sim$8.6 mag in the visual. The spectral energy distribution of the continuum shows a strong nebular component in the optical/near-UV region (Contini 1997). Also the Balmer jump in emission (see Fig. 1 of Kenyon et al. 1993) demonstrates well the recombination process in AG Peg.

We re-analyzed all available radial velocity data covering more than 20 orbital cycles during 1945 – 1992 (cf. Merrill 1951, 1959; Cowley & Stencel 1973; Hutchings et al. 1975; Kenyon et al. 1993). The data set of 82 radial velocity measurements (one point, [41 618.74, -19.2], was omitted as a very strong continuum was superposed on the comparison spectrum; cf. Hutchings et al. 1975) yielded practically the same elements as already derived by Kenyon et al. (1993), but the time of spectroscopic conjunction was shifted by about 60 days (probably a misprint in the Kenyon's et al. paper). Therefore we adopt the ephemeris

$$JD_{\rm sp.conj.} = 2\,427\,664.2(\pm 10) + 812.6(\pm 1.8) \times E \qquad (4)$$

as the best timing of the inferior conjunction of the cool giant in AG Peg from our solution for a circular orbit.

From $\sim$1940 the LC developed a periodic wave-like variation (Meinunger 1983). The periodic variability has been very intensively studied. The real shifts of the observed minima from the predicted positions were often noted (Belyakina 1985; Luthardt 1984, 1989). As a result, many different periods ranging from $\sim$730 to $\sim$830 days were suggested (Kenyon et al. 1993 and references therein). Generally, the older data gave a longer period (e.g. Meinunger 1983) than the more recent observations (e.g. Fernie 1985). Fig. 6 shows the photographic and visual LCs from 1935. Characteristic points (mostly maxima and minima) were taken from Meinunger's (1983) photographic measurements, while the visual data represent smoothed AFOEV estimates available from CDS. Positions of the observed minima are listed in Table 4. Their ephemeris is

$$JD_{\rm Min} = 2\,427\,495.9 + 820.3(\pm 0.8) \times E. \qquad (5)$$

To confirm the real difference of the photometric period from the orbital one given by Eq. (4), we divided the data set of radial velocities into two parts: (i) The old data from 1945.8 to

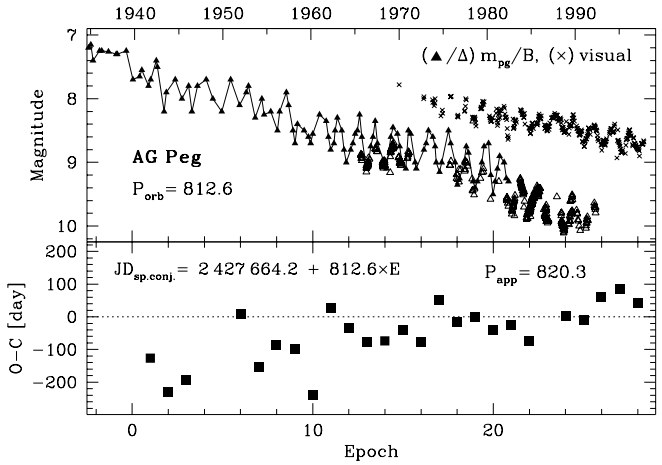

Fig. 6. Top: Compiled photographic/B and visual LCs of AG Peg as recorded from 1935. Bottom: The $O-C$ diagram for the observed minima. A gradual increase in the $O-C$ values indicates an apparent period of 820.3 days

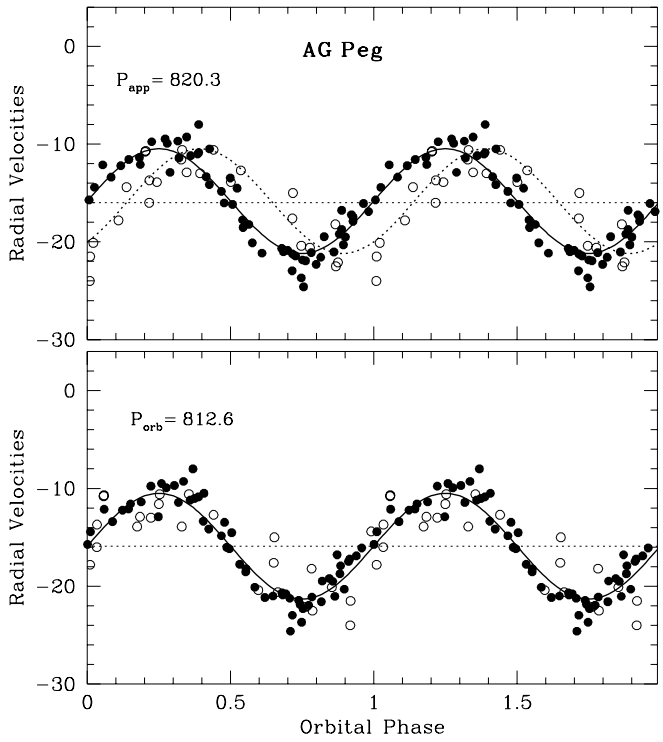

Fig. 7. Phase diagrams for the radial velocity measurements of AG Peg. Top: The 1945.8 - 1973.8 data (open circles) and the more recent, 1978.8 - 1992.0, measurements (full circles). The data sets are shifted by $\sim$0.15 $P_{\rm orb}$ relative to each other when folded with the photometric period of 820.3 days. Bottom: No systematic shift can be seen when the data are folded with the orbital period of 812.6 days (Eq. 4)

1973.8 (24 measurements), and (ii) the more recent data from 1978.5 to 1992.0 (58 measurements). Then we solved circular orbits for each data set separately with the fixed period of 820.3 days. Both solutions differ from each other only in the time of spectroscopic conjunction corresponding to an average shift of

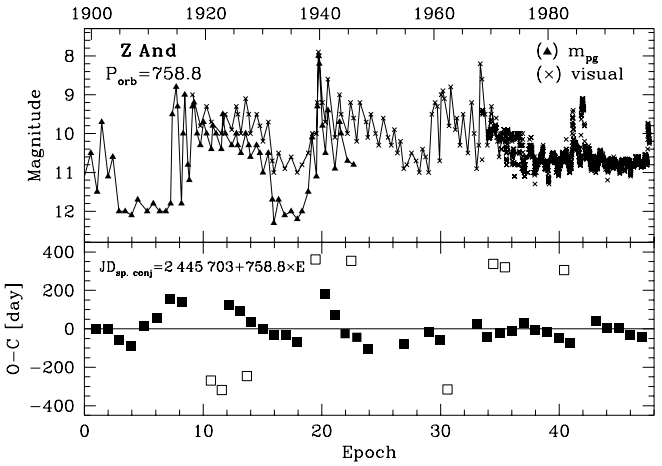

Fig. 8. Top: The historical LC of Z And. It is compiled from photographic data (Payne-Gaposchkin 1946), visual AAVSO estimates (Mattei 1978) and smoothed visual AFOEV data. Bottom: The $O-C$ diagram for the minima in Table 5

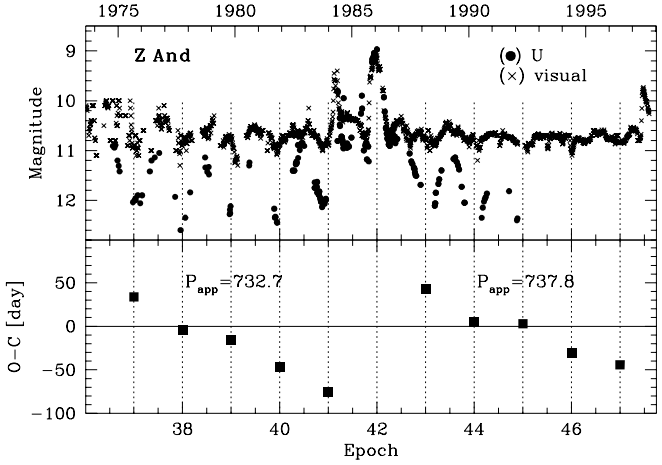

Fig. 9. Top: The U and visual LCs of Z And during the recent active phases. Bottom: The $O-C$ residuals indicate apparent periods of 732.7 and 737.8 days

0.15 $P_{\rm orb}$ between them (Fig. 7 top). However, the phase diagram of all radial velocities constructed for the elements in Eq. (4) does not display any systematic shift (Fig. 7 bottom). This means that the photometric period is inconsistent with the orbital period, and represents an apparent period in the system. The $O-C$ residuals display a systematic increase along a gradual decrease of the star's brightness. Such behaviour reflects a longer apparent period than the orbital one as in the case of V1329 Cyg.

Z And ($P_{\rm orb}$=758.8 days): This system consists of an M3-M4 giant ($M_{\rm g} \sim 2\,{\rm M}_\odot$, $R_{\rm g} \sim 100\,{\rm R}_\odot$, $L_{\rm g} \sim 880\,{\rm L}_\odot$) and a hot component ($M_{\rm h} \sim 0.65\,{\rm M}_\odot$, $L_{\rm h} \approx 900 - 2\,500\,{\rm L}_\odot$, $T_{\rm eff} \sim 10^5$ K) surrounded by an ionized nebula (cf. Mikolajewska & Kenyon 1996; Fernandez-Castro et al. 1995; Nussbaumer & Vogel 1989). The inclination of the orbital plane is 47$\pm$12° (Schmid & Schild 1997b).

Table 5. Minima in the light curve of Z And

$JD_{\rm Min}$ -2 400 000	Type	Ref	Phase*	E	O-C*
15350	pg	1	0.999	1	-1.0
16110	pg	1	2.000	2	0.2
16810	pg	1	2.923	3	-58.6
17540:	pg	1	3.885	4	-87.4
18400:	pg	1	5.018	5	13.8
19200:	pg	1	6.072	6	55.0
20060	pg	1	7.206	7	156.2
20800	pg	1	8.181	8	137.4
22670	pg	1	10.645	11	-269.0
23380	pg	1	11.581	12	-317.8
23820	pg	1	12.161	12	122.2
24550	pg	1	13.123	13	93.4
24970	vi	2	13.677	14	-245.4
25250::	vi	2	14.046	14	34.6
25973	pg,vi	1,2	14.998	15	-1.2
26700	pg	1	15.957	16	-33.0
27460	pg	1	16.958	17	-31.8
28180:	pg	1	17.907	18	-70.6
29370::	pg	1	19.475	19	360.6
29950	pg,vi	1,2	20.240	20	181.8
30600	pg,vi	1,2	21.096	21	73.0
31260	vi	2	21.966	22	-25.8
31640::	vi	2	22.467	22	354.2
32000	vi	2	22.941	23	-44.6
32700	vi	2	23.864	24	-103.4
35000::	vi	2	26.895	27	-79.8
36580:	vi,pg	2,3,4	28.977	29	-17.4
37300	pv	4	29.926	30	-56.2
37800	vi	2	30.585	31	-315.0
39660	vi	2	33.036	33	27.4
40350	vi	2	33.945	34	-41.4
40730	vi	2	34.446	34	338.6
41130	vi	2	34.973	35	-20.2
41470	vi	2	35.421	35	319.8
41900	vi	2	35.988	36	-9.0
42701.4	UBV	5	37.044	37	33.6
43421.8	UBV	5	37.994	38	-4.8
44170::	UBV	5	38.980	39	-15.4
44898	UBV	5	39.939	40	-46.2
45250	vi,V	6,5	40.403	40	305.8
45627	vi,UBV	6,5	40.900	41	-76.0
47263.8	UB	5	43.057	43	43.2
47985	vi,UBV	6,5	44.007	44	5.6
48741	vi	6	45.004	45	2.8
49467	vi	6	45.960	46	-30.0
50211.6	vi	6	46.942	47	-44.2

References: 1 - Payne-Gaposchkin (1946), 2 - Mattei (1978), 3 - Romano (1960), 4 - Mjalkovskij (1977), 5 - Belyakina (1985), 6 - from the AFOEV data on CDS. $\star$ $JD_{\rm sp.conj.}$ = 2 445 703 + 758.8×E

The nebular, hydrogen-recombination radiation dominates the near-UV/optical spectrum during both the quiescent and active stages (see Figs. 6 and 8 of Fernandez-Castro et al. 1988 and 1995, respectively). A broadening of all the emission line profiles in the recent, 1984-85, activity indicates an ejection of a shell at moderately high velocities of ∼200-300 km s^{-1}. The attenuation of the far-UV continuum due to Rayleigh scattering has only been detected during bright stages (Fernandez-Castro et al. 1995).

Based on all available M-type radial velocities, Mikolajewska & Kenyon (1996) derived the ephemeris for the time of inferior conjunction of the giant as

$$JD_{\rm sp.conj.} = 2\,445\,703.0 + 758.8(\pm 2) \times E, \quad (6)$$

which we also use in our paper, assuming that the period of 758.8 days represents the orbital one.

A complex wave-like modulation of the LC is indicated in quiescence as well as active stages throughout the whole observational period of Z And. As a result, more different periods have been suggested. For example, Payne-Gaposchkin (1946) obtained a mean period of 694 days, Belyakina (1985) suggested a period of 700 days and Kenyon & Webbink (1984) derived a 756.85-day period. Recently, Formiggini & Leibowitz (1994) analyzed all available photometric observations in the last 98 years. They found a sample of periods between 610 and 865 days, among which that of 759 days was suggested to be the orbital period and that of 656 days was present during high stages of activity. Fig. 8 shows the compiled photographic/visual LC as recorded from the beginning of this century. Timing of the observed minima are listed in Table 5. The $O-C$ values depend on the activity of the system. An abrupt change in the star's brightness, as in 1915, 1940 and 1984 ($Q \rightarrow A$ transitions), causes a significant change by a jump in the $O-C$ residuals to positive values, i.e. a larger period is indicated, while the $A \rightarrow Q$ transition is followed by a gradual decrease in the $O-C$ quantities indicating a shoter period than the orbital one. Fig. 9 illustrates such behaviour for the recent active phases. Apparent periods of 732.7 and 737.8 days correspond to the minima in the $A \rightarrow Q$ transitions, while the separation between the minima just preceding (E=41) and following (E=43) the activity in 1984-85 corresponds to a period of 818 days. However, all the primary minima from Table 3 (such that $|O-C|$ <182 days) yield the ephemeris as

$$JD_{\rm Min} = 2\,414\,625.2 + 757.5(\pm 0.5) \times E,$$

in which the average period is identical (within its uncertainty) with the orbital one in Eq. (6).

AG Dra ($P_{\rm orb}$=550.8 days): This symbiotic system is composed of a K-type (bright) giant ($M_{\rm g} \sim 1.5\,{\rm M}_\odot$) and a hot compact star, which could be a white dwarf ($M_{\rm h} \sim 0.4 - 0.6\,{\rm M}_\odot, L_{\rm h} \approx 1 - 5 \times 10^3\,{\rm L}_\odot, T_{\rm eff} \sim 1 - 1.5 \times 10^5$ K) embedded in a dense nebula (Mikolajewska et al. 1995). There are no signs neither in the optical nor far-UV regions of eclipses. Recently Schmid & Schild (1997a), based on spectropolarimetric observations, derived the orbital inclination $i = 60\,(\pm 8^\circ.2)$.

The system undergoes occasional eruptions, lasting about 1-2 orbital cycles. The star's brightness abruptly increases ($\Delta U \sim 2,\ \Delta V \sim$1 mag) showing multiple maxima separated approximately by 400 days (e.g. Luthardt 1983; Skopal 1995, 1998; Bastian 1998). During eruptions the hot component develops a fast wind at a few $\times 10^2$ km s^{-1} (e.g. Viotti et al. 1994a,

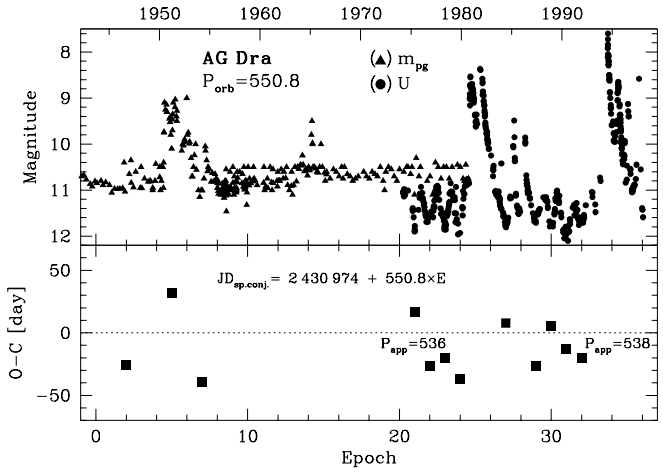

Fig. 10. Compiled photographic/U LC of AG Dra from ∼1940 (top). A fast $A \rightarrow Q$ transition produces a rapid change in the $O-C$ residuals (bottom)

Table 6. Minima in the light curve of AG Dra

JD_{Min} -2 400 000	Type	Ref	Phase*	E	O-C*
32050::	pg	1	1.954	2	-25.6
33760:	pg	1	5.058	5	32.0
34790:	pg	2	6.928	7	-39.6
42557.3:	U,pg	3,2	21.030	21	16.5
43064.8	U,u	3	21.951	22	-26.8
43622.4	U,u	3	22.964	23	-20.0
44156.3	U,u	3	23.933	24	-36.9
45853.4	U	3	27.014	27	7.8
46920.4	U	3	28.951	29	-26.8
47503.8	U	3	30.011	30	5.8
48035.8	U	3	30.976	31	-13.0
48579.4	U	3	31.963	32	-20.2

References: 1 - Sarov (1960), 2 - Luthardt (1983), 3 - Skopal (1994).
$\star$ $JD_{sp.conj.}$ = 2 430 974 + 550.8×E

1994b). The spectral energy distribution of the continuum shows a strong nebular component dominating the UV/optical region mainly during the activity (Fig. 5 of Greiner et al. 1997). The quiescent phase of AG Dra is characterized by a periodic wave-like variation in the optical continuum, which is more pronounced at short wavelengths (e.g. Skopal 1994).

Also in this case we re-analyzed radial velocity data as published by Mikolajewska et al. (1995), Smith et al. (1996) and Tomov & Tomova (1997). The dataset of 73 radial velocity measurements (one point, [49 376.6, -138.6], from the last dataset was omitted as it is deviated from other data by more than the semiamplitude of the whole variation) covering nearly 9 orbital cycles gave the elements very close (within their uncertainties) to those previously derived ($P = 550.8(\pm2.1)$ days, $e = 0.1$, $T_0 = 2\,431\,100.6$, $\omega = 0.07\,\mathrm{rad}$, $K = 5.0\,\mathrm{km\,s^{-1}}$, $\gamma = -148\,\mathrm{km\,s^{-1}}$). As a result we adopted the ephemeris

$$JD_{\mathrm{sp.conj.}} = 2\,430\,974(\pm10) + 550.8(\pm2.1) \times E \qquad (7)$$

as the best timing of the inferior conjunction of the cool component in AG Dra. Fig. 10 shows the m_{pg}/U LC from 1940 when AG Dra began to be active (cf. Friedjung 1988). The photographic LC was constructed from the data published by Luthardt (1983) in the same way as for AG Peg. The photoelectric measurements in the U/u bands represent those summarized by Skopal (1994). Positions of the observed minima are listed in Table 6. They obey the ephemeris

$$JD_{\mathrm{Min}} = 2\,430\,963.6 + 550.7(\pm0.4) \times E,$$

which is very close to that derived from radial velocities. Thus the orbital period can be considered to be 550.8 days. The $O-C$ residuals display rather short-term fluctuations, lasting a few periods. We can recognize apparent periods of 515 (E=5-7), 536 (E=21-24) and 538 days (E=30-32).

YY Her (P_{orb}=592.8 days): There is no detailed study on this object. Previous investigations showed that YY Her consists of a normal M3 giant (Kenyon & Fernandez-Castro 1987) and a hot compact star, $L_{\mathrm{h}} \approx 1\,100\,\mathrm{L}_\odot$, $T_{\mathrm{eff}} \sim 10^5$ K (Mürset et al. 1991). Spectroscopic observations revealed a strong emission line spectrum of HI, HeI, HeII and [OIII] (Herbig 1950). Munari (1997) showed that during the 1993 active phase the total integrated flux of all emissions dramatically increased. At that time the hot continuum dominated the optical spectrum (up to 7 500 Å) displaying a prominent Balmer jump in emission. Munari et al. (1997) summarized the historical LC from 1890 to 1996, showing that YY Her underwent several outbursts and/or bright phases. During quiescence, the continuum exhibits a complex wave-like modulation with a periodicity of ∼590 days (Munari et al. 1997).

Fig. 11 shows a part of the LC covering the period from its bright stage in 1971-74. Positions of the observed minima are compiled in Table 7. They determine the ephemeris as

$$JD_{\mathrm{Min}} = 2\,440\,637 + 592.8(\pm1.5) \times E. \qquad (8)$$

It is identical (within uncertainty) in the period with that of Munari et al. (1997), but differs from it in the initial epoch by 48 days. Thus we adopted elements in Eq. (8) for the purpose of this paper. The $O-C$ residuals display a large scatter, which, however, represents real variation in the minima position (see Fig. 11). For example, their systematic decrease from the 1971-74 brightening to the 1981-82 outburst, indicate an apparent period of ∼578 days. Also Munari et al. (1997) found the period to be ∼20 days shorter than 590 days prior to the 1981-82 active phase.

3.2. Common properties

There are two main characteristics in the variation of the $O-C$ residuals:

1. *Systematic variation in positions of the minima is connected with a variation in the energy distribution of the hot component radiation.*

The effect is very striking when also the nature of the hot continuum changes. In the case of eclipsing systems, the broad minima (i.e. those appearing during the nebular phase when the

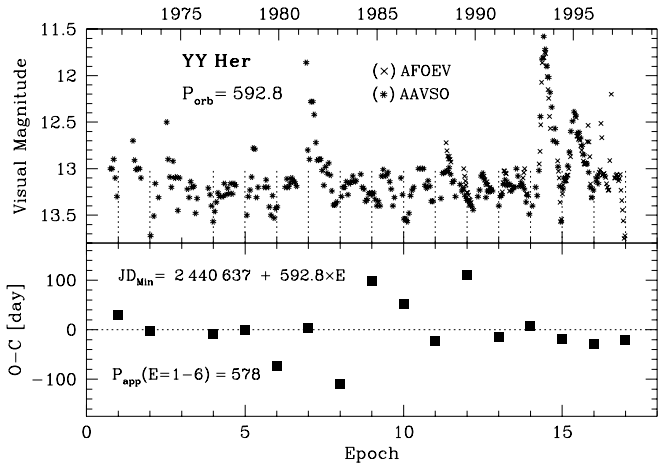

Fig. 11. Visual LC of YY Her from the 1971 bright phase. The AAVSO data set was taken from Munari et al. (1997), and the AFOEV data represent means in 30-day bins with a step width of 15 days. The $O-C$ residuals reflect a larger scatter as can be seen directly from changes in the positions of minima

Table 7. Minima in the light curve of YY Her

JD_{Min} -2 400 000	Type	Ref	Phase*	E	O-C*
41260::	vis	1	1.051	1	30.2
41820::	vis	1	1.996	2	-2.6
43000	vis	1	3.986	4	-8.2
43600::	vis	1	4.998	5	-1.0
44120:	vis	1	5.876	6	-73.8
44790	vis	1	7.006	7	3.4
45270	vis	1	7.815	8	-109.4
46070::	vis	1	9.165	9	97.8
46617.7	vis	1	10.089	10	52.7
47136.1:	vis	1	10.963	11	-21.7
47862.5	vis	1,2	12.189	12	111.9
48330:	vis	1,2	12.977	13	-13.4
48945:	vis	1	14.015	14	8.8
49511	vis	2	14.970	15	-18.0
50095	vis	1,2	15.955	16	-26.8
50695	vis	2	16.967	17	-19.6

References: 1 - from data published by Munari et al. (1997) 2 - from the AFOEV data on CDS
$\star$ JD_{Min} = 2 440 637 + 592.8×E

recombination radiation dominates the optical spectrum) occur *prior to* the time of spectroscopic conjunction. Contrary, when the ionized region is disrupted by eruption, the position of the minimum returns to the conjunction time. For example: (i) In BF Cyg the time of inferior conjunction of the giant star is indicated by a deep *narrow* minimum (the eclipse) at the epoch E=49. Both the subsequent and the preceding minima occurred before the time of spectroscopic conjunction (cf. Fig. 1, Table 1). A significant change in the nature of the optical continuum during the $A \rightarrow Q$ transition (E=49 to 51) – from a black-body to a nebular radiation – is well documented by the spectroscopic observations (Sect. 3.1; Fernandez-Castro et al. 1990; Skopal et al. 1997). (ii) The case of CI Cyg is qualitatively the same as that of BF Cyg. During the nebular phase of the $A \rightarrow Q$ transition (E=40–42) the broad minima also appeared prior to the spectroscopic conjunction of the giant (Fig. 3, Table 2). The variation in the hot component radiation in the optical during this transition is of the same nature as in BF Cyg (see Sect. 3.1). The return of the recent minima (E=44, 45) to the position of the conjunction predicted by Eq. (2) is again followed by a narrowing of their profile (Fig. 3). (iii) The nebular phase of V1329 Cyg has developed immediately after the 1964 eruption. The first well observed minimum occurred $\sim$80 days prior to the time of conjunction predicted by Eq. (3). All the subsequent minima also preceded the conjunction time, gradually approaching to it along a decline in the star's brightness, and thus causing a larger apparent period then the orbital one. (iv) Similar behaviour is observed in AG Peg, although we do not have a direct sign of eclipses in this system. At the beginning of its nebular phase, when the wave-like variation developed in the LC, from $\sim$ 1940, the minima were shifted by about -100 to -200 days from their prediction by Eq. (5), and were appearing systematically closer to the time of conjunction resulting in a larger apparent period. Also here such behaviour in the $O-C$ residuals is followed by a gradual decline of the star's brightness.
(v) In the case of non-eclipsing systems (Z And, AG Dra) the minima occur on both sides of the position of spectroscopic conjunction. The $O-C$ residuals generally move from positive to negative values during $A \rightarrow Q$ transitions.

2. *Separation between the minima correlates with the velocity of the brightness variation.*

Generally, a fast and large change in the period is indicated during $Q \rightarrow A$ transitions, when the brightness changes rapidly. Contrary, $A \rightarrow Q$ transitions, during which the star's brightness declines slowly, produce a smaller change in the period. To demonstrate this better, we determined a relation between parameters $\Delta m/\Delta t$ and $\Delta P/P_{\rm orb}$ characterizing the velocity of the change in the star's brightness and the corresponding phase shift in the period, respectively, for different transition epochs. The result is compiled in Table 8 and plotted in Fig. 12. The empirical relation

$$\frac{\Delta P}{P_{\rm orb}} \sim 134 \frac{\Delta m}{\Delta t} \qquad (9)$$

fits the data quite well. The parameter $\Delta m/\Delta t$ is in mag/day (see Table 8).

4. Interpretation

*4.1. Asymmetric shape of the H*II zone

The shape and position of a minimum in the LC reflect the geometry and location, respectively, of the main source of the optical continuum in binary. As the nebular radiation dominates the optical continuum during quiescence, but significantly changes during active phases, the observed photometric variations have to be caused mainly by changes of the ionization structure in symbiotic binary due to outbursts. It is intuitively clear that to

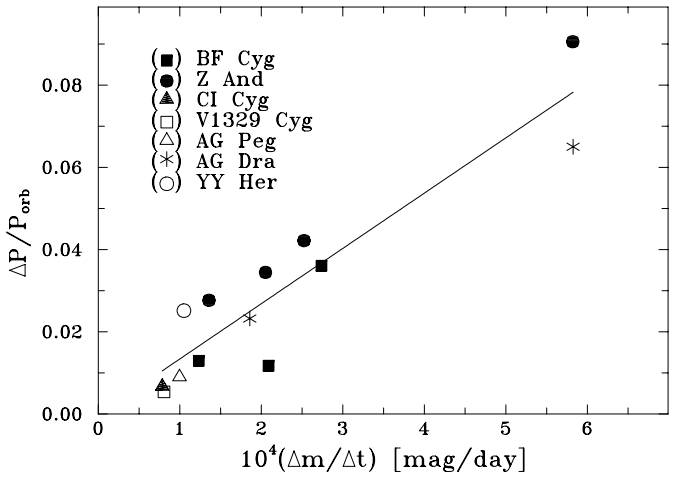

Fig. 12. Correlation between the velocity of the change in the star's brightness ($\Delta m/\Delta t$) and the corresponding phase shift in the period ($\Delta P/P_{\rm orb}$) for different transition epochs. The solid line represents a best linear fit given by Eq. (9)

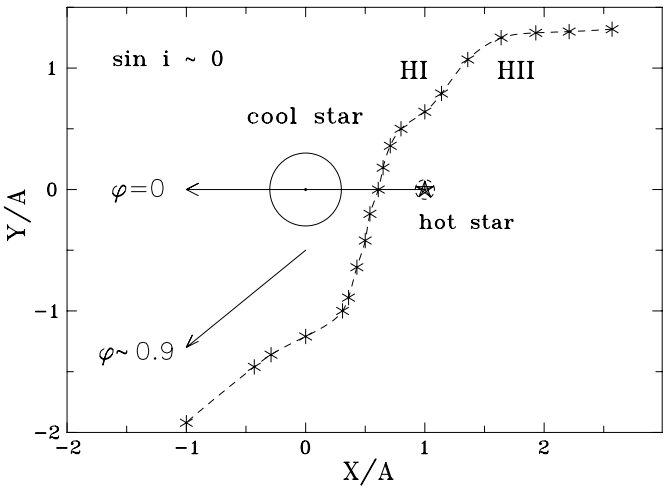

Fig. 13. Sketch of the inner part of ionization structure in symbiotic binary as viewed "pole-on" ($\sin i \sim 0$). The shape of the HI/HII boundary (asterisks connected by dashed line) is inspired by hydrodynamical calculations of Walder (1995, Fig. 3). It is probable that the optically thick part of the HII region also follows such a twisted pattern. This causes that the minimum of the nebular light occurres *prior to* spectroscopic conjunction (at $\varphi \sim 0.9$). However, when the optical light shifts to the hot star pseudophotosphere, as often observed during outbursts, the minima occur *at* the time of spectroscopic conjunction ($\varphi = 0$). The binary rotates anticlokwise

Table 8. Parameters of selected transition epochs. Quantities in the last two columns are factor of 10^2 and 10^4, respectively, enlarged

Object	E	Δt	Δm	$P_{\rm app}$	$\frac{\Delta P}{P_{\rm orb}}$	$\frac{\Delta m}{\Delta t}$
		day	mag	day		
BF Cyg	12-14	8930	1.1	747.5	1.29	1.23
	15-24	6720	1.4	748.4	1.18	2.09
	49-51	1461	0.4[a]	730.0	3.60	2.74
CI Cyg	39-42	2547	0.2	849.1	0.720	0.785
V1329 Cyg	31-40	8688	0.7	963.2	0.540	0.805
AG Peg	1-28	22109	2.2	820.3	0.948	0.995
Z And	12-18	4360	1.1	726.8	4.22	2.52
	20-24	2750	1.6	690.0	9.06	5.82
	37-41	2926	0.6	732.7	3.44	2.05
	43-47	2947	0.4	737.8	2.77	1.36
AG Dra	5-7	1030	0.6	515.0	6.50	5.83
	30-32	1076	0.2:	538.0	2.32	1.86
YY Her	1-6	2860	0.3	577.9	2.51	1.05

[a] - corresponds to the nebular phase (E=50-51)

describe the observed apparent changes in the orbital period, we have to assume an asymmetrical shape of the HII zone with respect to the binary axis. At present there are some indications of such an ionization structure in symbiotic binaries. We briefly summarize them in the following three points.

(i) Direct observational evidence of an asymmetrical HI (and thus also HII) region is represented by a wide 'eclipse', lasting from the orbital phase ∼0.9 to ∼1.6, in the far-UV region caused by Rayleigh scattering in BF Cyg (Pereira & Landaberry 1996). Skopal et al. (1997) qualitatively interpreted this effect as a result of a larger accumulation of the neutral material from the giant wind in the front of the preceding side of the hot star than behind it due to the orbital motion.

(ii) Asymmetric shape of the ionization front is suggested by spectropolarimetric studies. For example, in Fig. 5 of Schild & Schmid (1996) and Fig. 8 of Schmid (1998), the geometry of the HII zone has no symmetry with respect to the binary axis to explain the observed polarization properties. In these models, due to the orbital motion, the ionization front in the orbital plane is twisted, going from the side of the hot star that precedes its orbital motion, through the line joining the components, to the front of the cool star against its motion.

(iii) Asymmetrical nebular geometry is also suggested by hydrodynamical calculations of the structure of stellar winds in symbiotic stars that include effects of the orbital motion. The recent models of Walder (1995) and Kuznecov et al. (1997) are characterized by the S-shaped wind-collision zone, placed in the binary likewise as the ionization front described in the point (ii). This interaction region coincides with a large density which suggests that the ionization front follows this S-shaped pattern and probably represents the main part of the optically thick source of the continuum. However, no calculations confirming the latter speculation have been done.

Therefore we will assume that the shape of the optically thick portion of the HII region is prolonged in a direction between the stars and its projection into the orbital plane is inclined relatively to the binary axis by a phase angle $\Delta\varphi = 360 \times (\Delta P/P_{\rm orb})$. A sketch of this situation, inspired by hydrodynamical calculations of Walder (1995), is shown in Fig. 13. Such the region can be responsible for the minima in LC which are complex in shape and shifted from the time of spectroscopic conjunction.

4.2. Principle of apparent orbital changes

Variation in the ionization structure can, generally, be produced by variation in the luminosity of the ionizing photons, in the

mass loss rate from the giant and by interactions in the system. The first possibility is well documented by observations as described in Sect. 3. For the sake of simplicity, here we do not consider the variations in the mass loss rate and effects of interactions in the binary. Basically, there can be recognized two different sources of the hot continuum in the symbiotic system – a relatively cool and small pseudophotosphere around the hot component and the extended asymmetrical HII zone – dominating the optical spectrum during active and quiescent phases, respectively (Sects. 1, 3; Fig. 13). According to this fact, during outbursts we can observe deep narrow minima – eclipses – at the position of the spectroscopic conjunction, while during quiescence the minima are broad, complex in profile, and shifted from the position of the spectroscopic conjunction. The eclipsing systems, in which a pseudophotosphere around the hot component developes during eruptions (here BF Cyg and CI Cyg), represent best examples for understanding the basic principle of our interpretation (Sect. 4.3 below; also Fig. 13). A systematic change in timing of the minima can occur also if only the luminosity of ionizing photons changes, without any creation of a cool pseudophotosphere around the hot star, because this also produces a systematic variation in the shape of the HII zone (here V1329 Cyg and AG Peg). However, the variation is not so drastic as can be observed in the former case. Generally, any change of the luminosity of photons capable ionizing hydrogen ($L_{\rm ph}$) during the $A \leftrightarrow Q$ transitions will produce a shift in the minima position, and thus the apparent change in the orbital period. We found that a rapid change in the luminosity causes a larger change in the minima position. The recombination process transforms variation in $L_{\rm ph}$ into the optical, and that is why we observe a correlation between the parameters $\Delta m/\Delta t$ and $\Delta P/P_{\rm orb}$ estimated for different transition epochs (see Sect. 3.2, Eq. 9, Fig. 12). On the other hand, no variation in $L_{\rm ph}$ (i.e. $\Delta m/\Delta t = 0$) should result in a constant position of the minima (i.e. $\Delta P = 0$) which is in agreement with the epmirical relation (9).

4.3. Application to investigated objects

A *gradual* decrease in the star's brightness results in a *systematic* variation of the structure of the HII region, which then produces the observed variation in the $O-C$ residuals and thus an apparent change in the period. Here we distinguish two situations: (i) A *decrease* of the total luminosity, as during nebular stages of V1329 Cyg and AG Peg (nature of the optical continuum is not changed), produces also a decrease in the luminosity of the hydrogen ionizing photons. This leads to a gradual shrinking of the HII zone, and thus the minimum can be expected to occur prior, but closer to the position of the spectroscopic conjunction than during the previous cycle. As a result a larger apparent period than the orbital one is observed. (ii) An approximately *constant* hot star bolometric luminosity during a gradual decrease of the star's brightness throughout the $A \rightarrow Q$ transitions of BF Cyg and CI Cyg, produces an increase in the luminosity of the ionizing photons as the temperature of the hot star increases (this changes the nature of the optical continuum). These conditions cause an expansion of the HII zone fitting gradually its prolonged shape. The light minima, contrary to the case (i), will occur prior to, but systematically further from the time of spectroscopic conjunction. As a result, a shorter apparent period than the orbital one is indicated, and the minima become broader. Contrary, during $Q \rightarrow A$ transitions in these objects a rapid decrease in the luminosity of the $L_{\rm ph}$ photons results in practical disappearance of the HII region, and a cool pseudophotosphere around the hot star is created. Therefore the minima – eclipses – are observed at the spectroscopic conjunction and a sudden apparent change in the period by jump is indicated.

The cases of Z And and AG Dra are more complicated by a strong hot component wind which developes during their eruptions. Such an additional supplement of material (i.e. emittors) will consume an excess of ionizing photons (their HII zones are *open* in quiescence) and thus create an increase of the nebular emission with an adequate schrinkage and changes of geometry of the HII zone. At transition into quiescence, HII regions return to their previous shapes as before eruptions. We observe the same trend in the $O-C$ residuals as for BF Cyg or CI Cyg: a jump to positive values and a gradual decrease caused by the $Q \rightarrow A$ and subsequent $A \rightarrow Q$ transition, respectively. However, what is the result of the projection of a wide and complex HII region into the line of sight in the systems with a low orbital inclination, is difficult to describe. First, a theoretical calculations of the structure of winds in symbiotic binaries considering a variable hot star wind should be performed.

5. Summary

Analysing positions of the minima in the historical LCs of selected symbiotic stars we found that:

1. The variation in the $O-C$ residuals is systematic and thus reflects an apparent change of orbital period.
2. This systematic variation is connected with a variation in the energy distribution in the hot star spectrum observed during transition periods between different levels of activity.
3. The phase shift in the period, $\Delta P/P_{\rm orb}$, correlates with the velocity of the brightness variation, $\Delta m/\Delta t$ (in mag/day) as $\Delta P/P_{\rm orb} \sim 134 \Delta m/\Delta t$

To express just the basic principle of the observed variation in orbital periods of symbiotic binaries, the following points are relevant:

1. The hydrogen recombination radiation dominates the optical continuum of symbiotic binaries containing hot and luminous compact stars. Its location, the HII zone, can occupy a significant part of the circumbinary environment.
2. The nebular emission varies as a function of orbital phase. This function (i.e. the profile of the LC) results from the projection of the optically thick portion of the HII nebulosity into the line of sight.
3. Due to the orbital motion and interactions of stellar winds the HII region has an asymmetrical shape – it is prolonged along a direction between the components, but inclined to the binary axis.

4. When the nebular radiation dominates the optical continuum (mostly during quiescent phases) then the asymmetrical shape of the HII region produces broad minima which occur prior to the time of spectroscopic conjunction. Contrary, when the stellar component of radiation coming from the hot star pseudophotosphere dominates the optical spectrum (during active phases of many symbiotics), the narrow and deep eclipses occur at the position of spectroscopic conjunction. This is best illustrated by eclipsing systems of BF Cyg and CI Cyg.
5. Generally, any variation in the luminosity of photons capable ionizing hydrogen during transition periods between different levels of activity results in an adequate variation of the shape and location of the main source of the optical light in the binary, which produces the observed variation in the minima position, and thus an apparent change in the orbital period.

Acknowledgements. The author would like to express his thanks to Horst Drechsel for reading the manuscript and commenting on it and the referee, Hans Martin Schmid, for valuable comments. This research has been supported through the Alexander von Humboldt foundation. The author acknowledges the hospitality of the Astronomical Institute, University of Erlangen-Nürnberg, in Bamberg.

References

Aller L.H., 1954, Pub. DAO Victoria, 9, 321
Arkhipova V.P., 1977, Perem. Zvezdy, 20, 345
Arkhipova V.P., Mandel O.E., 1973, IBVS 762
Arkhipova V.P., Ikonnikova N.P., 1989, Sov. Astron. Lett. 15, 60
Bastian U., 1998, A&A, 329, L61
Batten A.H., 1973, 'Binary and Multiple Systems of Stars', Pergamon press, Oxford, p. 83
Belyakina T.S., 1979, Izv. Krymsk. Astrofiz. Obs. 59, 133
Belyakina T.S., 1984, Izv. Krymsk. Astrofiz. Obs. 68, 108
Belyakina T.S., 1985, IBVS, No. 2698
Belyakina T.S., 1992, Izv. Krymsk. Astrofiz. Obs. 84, 49
Cassatella A., Fernandez-Castro T., Gonzalez-Riestra R., Fuensalida J.J., 1992, A&A, 258, 368
Contini M., 1997, ApJ, 483, 887
Cowley A.P., Stencel R., 1973, ApJ, 184, 687
Fernandez-Castro T., Cassatella A., Gimenez A., Viotti R., 1988, ApJ, 324, 1016
Fernandez-Castro T., Gonzalez-Riestra R., Cassatella A., Fuensalida J.J., 1990, A&A, 227, 422
Fernandez-Castro T., Gonzalez-Riestra R., Cassatella A., Taylor A.R., Seaquist E.R., 1995, ApJ, 442, 366
Fernie J.D., 1985, PASP, 97, 653
Formiggini L., Leibowitz E., 1994, A&A, 292, 534
Friedjung M., 1988, in: J. Mikolajewska et al. (eds.), 'The Symbiotic Phenomenon', IAU Coll. 103, Kluwer, Dordrecht, p. 199
Ghedini S., 1982, 'Software for Photometric Astronomy', Willmann-Bell Publ. Comp., Richmond
Gonzalez-Riestra R., Cassatella A., Fernandez-Castro T., 1990, A&A, 237, 385
Greiner J., Bickert K., Luthardt R., Viotti R., Altamore A., González-Riestra R., Stencel R.E., 1997, A&A, 322, 576
Grygar J., Hric L., Chochol D., Mammano A.,1979, Bull. Astron. Inst. Czechosl., 30, 308
Herbig G.H., 1950, PASP, 62, 211
Hric L., Skopal A., Urban Z., et al., 1991, Contrib. Astron. Obs. Skalnaté Pleso, 21, 303
Hric L., Skopal A., Urban Z., et al., 1993, Contrib. Astron. Obs. Skalnaté Pleso, 23, 73
Hric L., Chochol D., Komžík R., 1993, Ap&SS, 201, 107
Hutchings J.B., Cowley A., Redman R.O., 1975, ApJ, 201, 404
Jacchia L., 1941, Bull. Harv. Coll. Obs. No. 915
Kenyon S.J., Webbink R.F., 1984, ApJ, 279, 252
Kenyon S.J., Fernandez-Castro T., 1987, AJ, 93, 938
Kenyon S.J., Oliversen N.A., Mikolajewska J., Mikolajewski M., Stencel R.E., Garcia M.R., Anderson C.M., 1991, AJ, 101, 637
Kenyon S.J., Mikolajewska J., Mikolajewski M., Polidan R.S., Slovak M.H., 1993, AJ, 106, 1573
Kuznetzov O.A., Bisikalo D.V., Boyarchuk A.A., Chechetkin V.M., 1997, in: J. Mikolajewska (ed.), Physical Processes in Symbiotic Binaries, Copernicus Foundation for Polish Astronomy, p. 71
Luthardt R., 1983, Mitt. Veränd. Sterne, 9, 129
Luthardt R., 1984, IBVS, No. 2495
Luthardt R., 1989, Veroff. Sterne Sonneberg, 10, 255
Mattei J.A., 1978, J. Roy. Astron. Soc. Can., 72, 61
Meinunger L., 1983, Mitt. Verand. Sterne, 9, 92
Merrill P.W., 1951, ApJ, 113, 605
Merrill P.W., 1959, ApJ, 129, 44
Mikolajewska J., 1997, in: J. Mikolajewska (ed.) 'Physical Processes in Symbiotic Binaries', Copernicus Foundation for Polish Astronomy, Warszaw, p. 3
Mikolajewska J., Mikolajewski M., 1983, Acta Astron., 33, 403
Mikolajewska J., Kenyon S.J., Mikolajewski M., 1989, AJ, 98, 1427
Mikolajewska J., Kenyon S.J., Mikolajewski M., Garcia M.R., Polidan R.S., 1995, AJ, 109, 1289
Mikolajewska J., Kenyon S.J., 1996, AJ, 112, 1659
Mjalkovskij M., 1977, Peremenye zvezdy, 3, 71
Munari U., 1997, in: J. Mikolajewska (ed.) 'Physical Processes in Symbiotic Binaries', Copernicus Foundation for Polish Astronomy, Warszaw, p. 37
Munari U., Margoni R., Mammano A., 1988, A&A, 202, 83
Munari U., Rejkuba M., Hazen M., et al., 1997, A&A, 323, 113
Mürset U., Nussbaumer H., Schmid H.M., Vogel M., 1991, A&A, 248, 458
Nussbaumer H., Schmutz W., Vogel M., 1986, A&A, 169, 154
Nussbaumer H., Vogel M., 1989, A&A, 213, 137
Nussbaumer H., Vogel M., 1991, A&A, 248, 81
Payne-Gaposchkin C., 1946, ApJ, 104, 362
Pereira C.B., Landaberry S.J.C., 1996, AJ, 111, 1329
Pucinskas A., 1970, Bull. Vilnius Univ. Astron. Obs. No. 27, 24
Romano G., 1960, Mem. Soc. Astr. It., 31, 11
Schild H., Schmid H.M., 1996, A&A, 310, 211
Schild H., Schmid H.M., 1997, A&A, 324, 606
Schmid H.M., 1998, Rev. in Mod. Astronomy, 11 (in press)
Schmid H.M., Schild H., 1997a, A&A, 321, 791
Schmid H.M., Schild H., 1997b, A&A, 327, 219
Seaquist E.R., Taylor A.R., Button S., 1984, ApJ, 284, 202
Skopal A., 1992, IBVS No. 3780
Skopal A., 1994, IBVS No. 4096
Skopal A., 1995, in: G. Balazs et al. (eds.), IAPPP Symp. 'CCD Techniques in Stellar Photometry', Arculat Press, Baja, p. 129
Skopal A., 1996, in: D. Chochol, A. Skopal, T. Pribulla (eds.) 'Physical Processes in Interacting Binaries', Astron. Institute SAV, Tatranská Lomnica, p. 53
Skopal A., 1998, in: M. Grenon, J. Mattei (eds.), 'Variable stars: New frontiers', Publ. Astron. Soc. Pacific, (in press)

Skopal A., Hric L., Urban Z., et al., 1992, Contrib. Astron. Obs. Skalnaté Pleso, 22, 131
Skopal A., Vittone A., Errico L., Bode M.F., Lloyd H.M., Tamura S., 1997, MNRAS, 292, 703
Smith V.V., Cunha K., Jorissen A., Boffin H.M.J., 1996, A&A, 315, 179
Stellingwerf R.E., 1978, ApJ, 224, 953
Stienon F.M., Chartrand M.R., Shao C.Y., 1974, AJ, 79, 47
Tomov N.A., Tomova M.T., 1997, in: J. Mikolajewska (ed.) 'Physical Processes in Symbiotic Binaries', Copernicus Foundation for Polish Astronomy, Warszaw, p. 185
Viotti R., González-Riestra R., Rossi C., 1994a, IAU Circ. 6039
Viotti R., Mignoli M., Comastri A., Bedalo C., Ferluga S., Rossi C., 1994b, IAU Circ. 6044
Walder R., 1995, in: K.A. van der Hucht & P.M. Williams (eds.), Wolf-Rayet Stars: Binaries, Collidings Winds, Evolution., IAU Symp. 163, p. 420